Environ. Sci. Technol. **2010,** *44,* 2386–2392

Biodegradation in a Partially Saturated Sand Matrix: Compounding Effects of Water Content, Bacterial Spatial Distribution, and Motility

ARNAUD DECHESNE,*,† MIKOŁAJ OWSIANIAK,† ALEXIS BAZIRE,‡,† GENEVIÈVE L. GRUNDMANN,§ PHILIP J. BINNING,† AND BARTH F. SMETS†

Department of Environmental Engineering, Technical University of Denmark, Miljoevej Bg 113, 2800 Kgs. Lyngby, Denmark, and Université Lyon 1, IFR 41, CNRS, UMR5557, Ecologie Microbienne, Villeurbanne, F-69622, France

Received September 11, 2009. Revised manuscript received February 2, 2010. Accepted February 15, 2010.

Bacterial pesticide degraders are generally heterogeneously distributed in soils, leaving soil volumes devoid of degradation potential. This is expected to have an impact on degradation rates because the degradation of pollutant molecules in such zones will be contingent either on degraders colonizing these zones or on pollutant mass transfer to neighboring zones containing degraders. In a model system, we quantified the role exerted by water on mineralization rate in the context of a heterogeneously distributed degradation potential. Alginate beads colonized by *Pseudomonas putida* KT2440 were inserted at prescribed locations in sand microcosms so that the initial spatial distribution of the mineralization potential was controlled. The mineralization rate was strongly affected by the matric potential (decreasing rate with decreasing matric potential) and by the initial distribution of the degraders (more aggregated distributions being associated with lower rates). The mineralization was diffusion-limited, as confirmed with a mathematical model. In wet conditions, extensive cell dispersal was observed for the flagellated wild type and, albeit to a lesser extent, for a nonflagellated mutant, partially relieving the diffusion limitation. Dry conditions, however, sustained low mineralization rates through the combined effects of low pollutant diffusivity and limited degrader dispersal.

Introduction

There is mounting evidence that microbial pesticide degradation potential is most often heterogeneously distributed in soils. This is true in bioaugmented and nonbioaugmented soils. The current bioaugmentation technologies often rely on the inoculation of carriers such as clay (*1*) or alginate (*2*) that contain the degrading organisms. Even if these carriers are carefully mixed with surface soil, it is inevitable that, at least upon inoculation, degradation hotspots are created in and immediately around the carriers, leaving the remaining soil devoid of degradation potential. Similarly, if degraders are brought in a liquid suspension applied to the soil surface, significant spatial heterogeneity in the degrader distribution is expected, at least initially (*3*).

The situation is not fundamentally different in nonbioaugmented soils in which natural pesticide attenuation occurs. As with many other microbial parameters (*4–6*), pesticide degradation potential usually varies greatly in space within agricultural fields (*7–9*). It has nevertheless proven challenging to detect spatial scales of variability for pesticide mineralization and, a fortiori, to identify parameters that explain or covary with that type of microbial activity, although some basic parameters such as soil pH or C/N ratio were sometimes shown to be good predictors of mineralization rate (*9*). Some studies of spatial variability of pesticide mineralization have explored not only the field scale but also smaller scales (the so-called microscale, with distances between sampling points on the order of a few centimeters or smaller). The conclusion of such studies for 2,4-D degradation is that there exist volumes of soil of a few cubic centimeters that are devoid of significant degradation potential (*10, 11*). This is in line with the current view on microbial endemism in soil, according to which the former "everything is everywhere" paradigm is not true (*12*).

The problem posed by patchy spatial distributions of pesticide degraders has been identified (*3, 13, 14*): all pesticide applied or transported to volumes of soil that do not contain degraders will not be readily degraded. Before any degradation occurs, mass transfer needs to take place. There are many processes that can contribute to spatially redistribute either pesticide molecules or degrader cells. Among them soil biota such as fungal hyphae (*15*) or earthworms (*16*) and soil management such as tillage (*17*) can play a prominent role. Additionally, water flow caused by precipitation events or irrigation has the potential to transport pesticide molecules and bacteria toward deeper soil layers. It is not clear how much these convective flows also contribute to horizontal redistribution of cells and solutes in surface soils. Even in the absence of convective water flow, soil moisture is essential to the mass transfer of pesticide and degraders. Indeed, bacterial Brownian motion and active motility require liquid films of sufficient thickness (*18, 19*). Similarly, solute aqueous diffusion is directly impacted by soil moisture content because diffusion rate is a function of the liquid film thickness (*20*).

As a consequence, it is expected that in a context of a heterogeneously distributed degradation potential, pesticide degradation rate will be mediated by soil−water content through its control of pollutant and cell mass transfers. The objective of this work was to quantify the role of the spatial distribution of degraders on the mineralization rate of a substrate as affected by water content (matric potential). In order to isolate these processes, we chose an approach based on microcosms for which the initial conditions can be controlled. A number of key parameters were prescribed at the onset of the mineralization experiments: the abundance and spatial distribution of degrader cells, concentration and distribution of the model degradable soluble compound (benzoate), and matric potential of the porous medium.

Materials and Methods

Degrading Strains. We used a derivative of *Pseudomonas putida* KT2440 that constitutively expresses the green fluorescent protein (GFP) (*3, 18*) as a model benzoate-

* Corresponding author phone: +45 45 25 22 91; e-mail: ard@env.dtu.dk.
† Technical University of Denmark.
‡ Present address: Université de Bretagne Sud, Laboratoire de Biotechnologie & Chimie Marine, 56321 Lorient Cedex, France.
§ Université Lyon 1.

10.1021/es902760y

Published on Web 03/01/2010

degrading strain. This organism was deemed a relevant model because its parental strain was isolated from soil (*21*) and because its motility under unsaturated conditions has been studied previously (*18*). Because of its physicochemical properties, benzoate can be considered a good analogue to many commonly used ionic pesticides such as 2,4-D, dicamba, or fluoroxypyr (Supporting Information). A GFP-tagged, nonflagellated isogenic mutant of KT2240 was created by allelic exchange with a truncated version of *fliM* carrying the Gm-resistance gene *aacC1* framed by *lox* sequences. The *aacC1* gene was then excised to yield an antibiotic-resistance free mutant (*22*) (see Supporting Information for more details on the procedure). Unlike KT2440 wild-type, the Δ*fliM* mutant is unable to swim, as verified in soft agar and by microscopy (data not shown). These strains were maintained on FAB minimal medium supplemented with 5 mM benzoate as the sole carbon source. The FAB medium is composed of [in mM]: $MgCl_2$ [1], $CaCl_2$ [0.1]; Fe-EDTA [0.01], $(NH_4)_2SO_4$ [15], Na_2HPO_4 [33], KH_2PO_4 [22], and NaCl [51] (*23*).

Alginate Beads. To introduce degraders at specific locations in the microcosms, we embedded the cells in alginate beads using a protocol adapted from ref *24*. Briefly, 5 mL of a fresh culture with an $OD_{600\ nm}$ of about 0.3 was mixed with 45 mL 3% (w/v) alginate sodium. After 1 h of stirring, a few milliliters of this mixture were added dropwise to a gently stirred 0.1 M $CaCl_2$ solution. After 2 h of hardening, the beads were removed and transferred into 1/4 strength LB medium for an overnight incubation that allowed full colonization of the beads. The beads were then rinsed twice with saline solution and drained before being introduced in a microcosm within the same day. The beads were about 2 mm in diameter and contained on average 1.29×10^6 CFUs (s.d. 5.4×10^5 CFUs).

Microcosms and Mineralization Measurements. The microcosms consisted of about 50 cm^3 of sand (75 g dry sand) placed in an autoclavable cylindrical plastic jar (4 cm in diameter, 3.7 cm in height). Quartz sand (−50 +70 mesh, Sigma Aldrich, St Louis, MO) was preferred to soil because a soil would have contained substrates other than the benzoate amendment, potentially interfering with bacterial metabolism and motion. Additionally, this sand has a well-defined particle size distribution and has previously been used in microbial ecology research (*25*). The sand was rinsed with deionized water, dried, and autoclaved. Then, the dry sand was brought to the correct matric potential (−1, −8, or −50 kPa) by adding the appropriate quantity of liquid (0.2, 0.08, or 0.02 g liquid per g of dry sand, respectively (*25*)). The solution added was composed of FAB medium and of C^{14}-ring-labeled benzoate. The aqueous concentrations of the mineral components of the medium (FAB) were the same in all microcosms, but the concentration of benzoate was varied in order to maintain a benzoate load of 5 mg kg^{-1} dry sand, irrespective of the matric potential. Similarly, the C^{14} activity was adjusted to 667 DPM g^{-1} dry sand (about 50000 DPM per microcosm). To homogenize the moisture content and benzoate concentration, we aseptically stirred the batches of sand after the addition of liquid and left them to equilibrate for four days. The microcosms were then constructed by sequentially adding portions of amended sand in the plastic jars and inserting nine alginate beads, according to three prescribed spatial distributions. The nine beads were either all placed in the center of the microcosm (single hotspot) or distributed into three hotspots (three beads each) or nine hotspots (Figure 1 of the Supporting Information).

The microcosms were individually placed in sealed 0.75 L glass jars, where a base trap (1.5 mL of 1 M KOH in a 20 mL vial) was placed to capture the evolved $^{14}CO_2$. To minimize sand drying, we added to the glass jar a container with 20 mL of a salt solution of water potential similar to that set for the microcosm (*26*). The base trap was sampled and replaced by fresh KOH solution from once every two days to once every two weeks, depending on the mineralization rate. The microcosms were weighed, and any evaporative loss was compensated by carefully adding drops of sterile deionized water on the top of the microcosms. To measure the quantity of evolved $^{14}CO_2$, we mixed the content of the base trap with 10 mL of scintillation liquid (OptiPhase HiSafe 3, PerkinElmer, Waltham, MS) and analyzed it by scintillation counting. For each microcosm the mineralization experiment was terminated when two consecutive measurements of evolved $^{14}CO_2$ were in the range of the detection limit of the scintillation counter. Between 3 and 6 replicate microcosms were constructed per treatment (a combination of matric potential and spatial distribution).

Spatial Dynamics of Cells in Sterile Sand. The dispersal of the cells from their inoculation point was studied in the microcosms constructed with a single central bacterial hotspot. After having removed the lid of the plastic jar at the bottom of the microcosm, depth slices of the microcosm were sequentially sampled by gently pushing the sand cylinder out of its plastic jar, bottom first, and cutting sections with a flamed scalpel. Five to six slices were cut from the bottom half of the microcosms. Each of the slices was weighed and suspended in sterile saline solution. Serial dilutions of these suspensions were then plated on a FAB−benzoate solid medium to enumerate cultivable cells.

This sampling was performed at the end of the mineralization experiment on duplicate microcosms incubated at −8 and −50 kPa. Later, new duplicate microcosms were constructed, incubated at −8 kPa, and sacrificially sampled after 3, 7, or 21 days.

Modeling. A model was developed in COMSOL Multiphysics (COMSOL, Burlington, MA) that describes the three-dimensional (3-D) diffusion-driven mass transfer of the pollutant within the sand matrix and its mineralization in the degrader hotspot(s). Benzoate metabolism was supposed to follow Monod kinetics, and biomass was restricted to the hotspot(s). As in the experiments, one, three, and nine degradation hotspots were spatially distributed within a cylindrical domain. To calculate benzoate effective diffusivity as affected by hydration conditions, we used a simple power function model (*27*) (see Supporting Information for details on model and simulations).

Results

Extent of Mineralization. The percentage of radioactivity introduced as ^{14}C-benzoate that was recovered as $^{14}CO_2$ at the end of the experiments varied between 51% and 105%, with an average of 79% (data not shown). A two-way ANOVA revealed significant differences in the mineralization extent between some treatments, but no clear interpretation was apparent (i.e., no gradient in mineralization extent could be linked to the prescribed gradients of moisture or degrader distribution).

Mineralization Rate. The kinetics of $^{14}CO_2$ evolution revealed an effect of matric potential on mineralization rate, with faster mineralization associated with moister sand (Figure 1). While the mineralization plateaued in less than one week at −1 kPa and in two to three weeks at −8 kPa, it took more than 19 weeks at −50 kPa. In addition to the effect of moisture, an effect of the spatial distribution of the degraders at inoculation was also clear: for each matric potential, the mineralization was always faster in the microcosms containing more hotspots.

For most treatments, the initial part of the mineralization curves (before about 60% of the final mineralization extent was reached) was approximately linear (Figure 1). Linear regressions were performed on this part of the curves, and estimates of the slopes were used as a metric of the mineralization rate (Table 1).

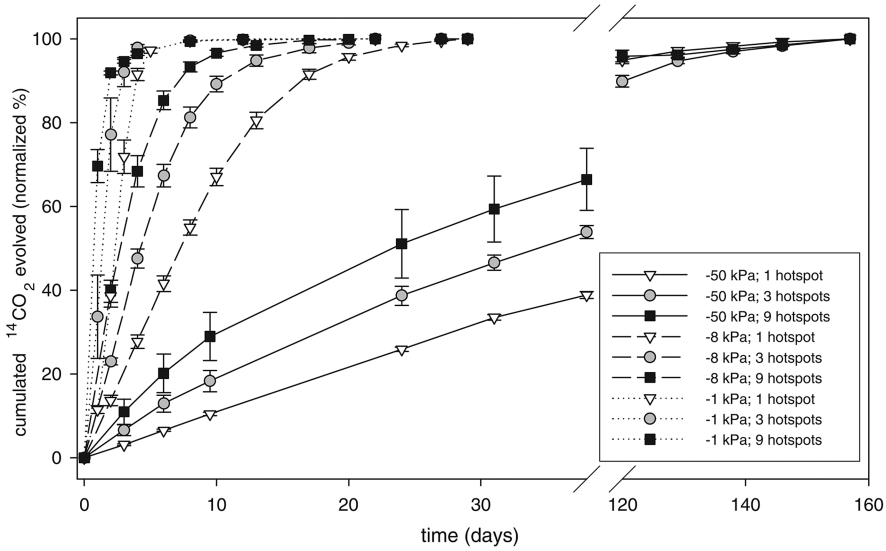

FIGURE 1. Effect of sand moisture and degrader spatial distribution on benzoate mineralization rate. To make the graph more legible, we normalized the cumulated radioactivity values for each microcosm by the final value (i.e., the final point is 100% for each microcosm). However, note that all analyses in the text were performed on non-normalized data. Average values for each time point and treatment are plotted (three to four replicates), with the standard error of the mean serving as the error bar. More replicate experiments were performed but are not integrated into this graph because the microcosms have been sampled at different times, making general averaging impossible.

TABLE 1. Initial Mineralization Rates for Different Sand Moistures and Degrader Spatial Distributions (*P. putida* KT2440 or Its Nonflagellated Mutant)[a]

	spatial distribution (number of hotspots) at inoculation					
matric potential (kPa)	**1**		**3**		**9**	
wild type						
−50	0.98	(0.01)	1.71	(0.05)	2.54	(0.21)
−8	4.53	(0.11)	10.14	(0.17)	13.81	(0.86)
−1	12.47	(0.71)	29.22	(3.00)	64.58	(3.50)
Δ*fliM* mutant						
−8	3.82	(0.04)	7.36	(0.26)	12.91	(0.40)

[a] The rates derive from the slope of the initial part of the mineralization curves. They are expressed as percentages of the total radioactivity introduced in the microcosms as ^{14}C-benzoate mineralized per day. Standard errors are in parentheses.

These values capture succinctly how an increased moisture content and higher number of degrader hotspots were conducive to faster mineralization, with a ratio of fastest (−1 kPa, nine hotspots) to slowest (−50 kPa, one hotspot) mineralization of 65.

Subsequently, a mineralization experiment was conducted at −8 kPa with the nonflagellated mutant (Δ*fliM* mutant). The mineralization curves suggest the mutant did not mineralize benzoate as fast as the wild type (Figure 2). The estimated initial mineralization rates associated with the mutant were significantly smaller ($P < 0.05$) than those observed with the wild type (Table 1). Albeit modest in absolute values, these differences represent a reduction by 16%, 27%, and 6% from the values observed with the wild type for one, three, and nine hotspots, respectively.

Cell Dispersal. The sacrificial sampling of the microcosms at the end of the experiments revealed that matric potential strongly influenced cell dispersal. While for the microcosms incubated at −8 kPa for 4 weeks many KT2440 cells were found in the bottommost slice (more than 1.2 cm from the inoculation point), cells in microcosms incubated at −50 kPa for 35 weeks were found only in the vicinity of the inoculation point (data not shown).

The kinetics of cell dispersal was studied in microcosms incubated at −8 kPa (Figure 3). Despite the variability between replicates, the data indicate a rapid cell dispersal because cells were found at more than 0.6 cm from the inoculation point after three days of incubation. After one week, the microcosms were uniformly colonized with the abundance of cultivable cells exceeding 8×10^5 CFU per g of dry sand, irrespective of depth. By contrast, the nonflagellated derivative of KT2440 displayed a delayed colonization pattern (Figure 3). If this was not obvious after three days, with a microcosm showing the presence of cells having dispersed over more than 0.8 cm, the delay was evident after one week, with an absence of cells in the bottommost samples. After three weeks, the bottom of the microcosms was colonized by the nonflagellated cells but with densities 2 orders of magnitude lower than that of the wild type.

Discussion

Diffusion-Limited Mineralization Rates. Matric potential was the main determinant of mineralization rate in our experiments, drier conditions being associated with lower rates (Table 1). It is most likely that the matric potential primarily affected mineralization through its control of benzoate effective diffusivity as predicted values are reduced 15-fold when the matric potential decreases from −1 to −50 kPa (Table S2 of the Supporting Information). Alternative effects of low matric potential are implausible in our

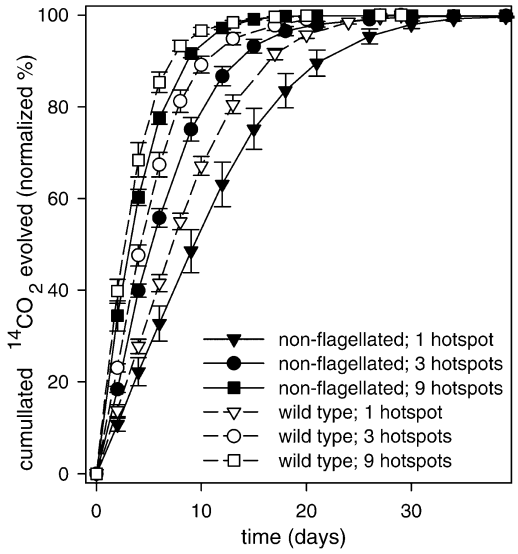

FIGURE 2. Effect of *P. putida* KT2440 initial spatial distribution and flagellation on benzoate mineralization rate in microcosms incubated at −8 kPa. To make the graph more legible, we normalized the cumulated radioactivity values for each microcosm by the final value (i.e., the final point is 100% for each microcosms). Average values for each time point and treatment are plotted (three to four replicates), with the standard error of the mean serving as the error bar.

experimental system. Indeed, even the driest condition used (−50 kPa) does not constitute a significant matric stress to the cells because adverse effects of matric potential on *Pseudomonas* physiology are observed at much more negative potentials (*28*). The initial aqueous concentration of benzoate was higher at low matric potential (2 mM at −50 kPa) than that at high matric potential (0.2 mM at −1 kPa), so that all microcosms contained the same mass of benzoate. A 2 mM benzoate concentration is moderate for KT2440, which is routinely grown on 5 mM benzoate in our laboratory. In stirred liquid medium, KT2440 is even expected to present faster mineralization rate at 2 mM than at 0.2 mM benzoate. In the microcosms, on the contrary, much faster rates were observed at −1 kPa than at −50 kPa, proving that benzoate aqueous concentration did not govern mineralization rate.

The mineralization was diffusion limited because each alginate bead contained a large mineralization potential that depleted benzoate in its direct vicinity quicker than it was replenished by diffusion. Therefore, the reduction of benzoate effective diffusivity associated with dryer conditions translated into stronger diffusion limitation and smaller mineralization rates. By contrast, the presence of several hotspots in the microcosms allowed the simultaneous exploitation of several spatially separated pools of benzoate, resulting in faster microcosm-wide mineralization. Diffusion limitation has been recognized as a common factor hindering in situ pollutant removal (*29*) and has been directly observed for naphthalene degradation in simplified experimental systems (*30*).

The prominent role of diffusion was confirmed by the predictions of a 3-D model that takes into account the distribution of bacterial hotspots and effective diffusivity of benzoate. The model indeed predicted that a change from −1 to −50 kPa results in a 1 order of magnitude reduction of the mineralization rate (Figure 4). However, Figure 4 also shows that model-predicted rates are much smaller than experimental ones, suggesting that the model did not capture the mass transfer processes in the microcosms satisfactorily. Because the experiments were designed so that mass transfer of benzoate was diffusive only (no water flow), the discrepancy most

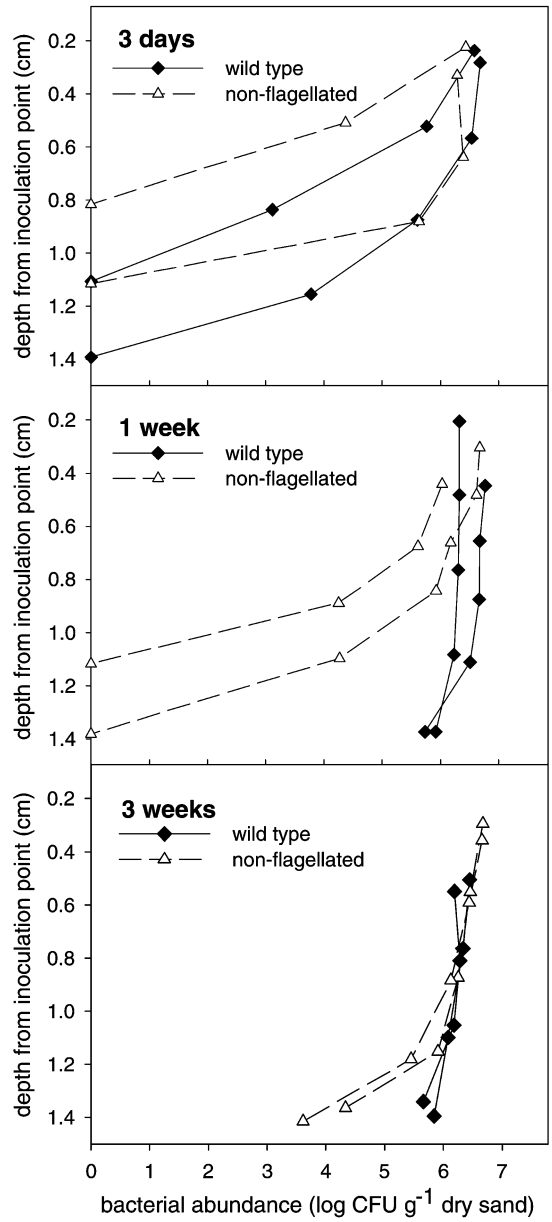

FIGURE 3. Spatial dynamic of KT2440 wild type and its nonflagellated mutant in microcosms maintained at −8 kPa. Data originate from sacrificial sampling of the bottom half of 12 microcosms, inoculated with either type of bacteria, and incubated for three days, one week, or three weeks. Depth 0 represents the microcosm center (inoculation point), and depth 1.5 cm represents its bottom.

probably originates from the "microbial" part of the model. However, because of diffusion limitation, modifying the microbial kinetic parameters toward a much faster potential benzoate metabolism (half saturation constant, *K*s, divided by 5 and maximum rate of substrate uptake per cell, q_{max}, multiplied by 5) did not improve the predictions (Figure S3 of the Supporting Information). This suggests that the discrepancy originates from a process not included in the model that partly relieves the diffusion limitation. We argue that this process is bacterial dispersal from the alginate carriers, which results in the reduction of the distance benzoate molecules need to diffuse before being degraded.

Cell Dispersal. Sacrificial sampling of the microcosms led to the detection of wild type cells several centimeters away from their inoculation point after a few incubation days at −8 kPa (Figure 3). Cells had thus been readily released

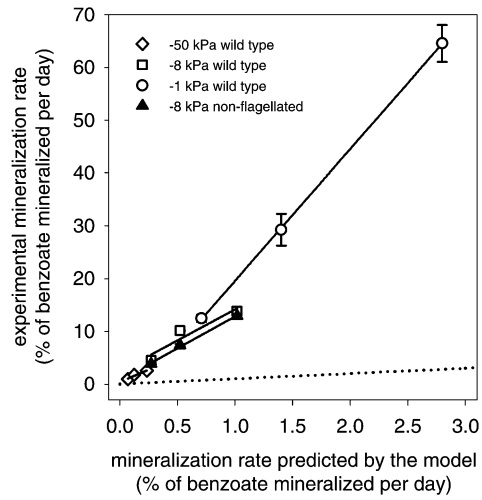

FIGURE 4. Comparison of experimentally derived and model-predicted benzoate mineralization rates as influenced by hotspot distribution, matric potential, and cell flagellation. A perfect agreement between model and experimental results would result in alignment of the data points on the first diagonal (discontinuous line).

from the beads before further dispersing in the matrix. This rapid release, previously mentioned in the literature (*31*), was probably favored by the fact that the beads were introduced into the microcosms within hours from their preparation, without extended drying. While we did not detect cells in the bottommost sections of the microcosms at the end of incubation at −50 kPa, it is probable that cells were also released and started to colonize in the direct vicinity of the beads. Growth is likely to have occurred because of the quantity of benzoate available in the microcosms (0.378 mg). Assuming a yield of 0.4 g of microbial C per g of benzoate C, a cell dry weight of 2.8×10^{-13} g and $C_5H_7O_2N$ as molecular formula for biomass, then we calculate that about 6×10^8 cells could have been synthesized if all the benzoate was consumed. The high microbial abundances measured in the bottom of the microcosms incubated at −8 kPa (Figure 3) certainly partly result from local growth. The release from the beads and subsequent growth would have led, in dry conditions, to a limited colonization of the sand matrix (e.g., a few millimeters from the bead), enlarging the mineralization hotspot(s), thus reducing diffusion limitation. This hypothesis was explored by doubling the radius of the mineralization hotspot(s) in our model. While reasonable agreements between experiments and simulations were obtained at −50 kPa, the model still underestimated the mineralization rates in wetter conditions (Figure S3 of the Supporting Information). This underestimation is attributed to the fact that under wet conditions cells rapidly dispersed much farther than a few millimeters away from the beads. This was demonstrated here at −8 kPa (Figure 3) and must have happened even faster at −1 kPa due to the increased water content (*19*).

The threshold for extensive cell dispersal was between −8 and −50 kPa. This is consistent with the results of Treves and collaborators (*25*), where in microcosms made of the same sand as the type used here, the spatial isolation of two competing bacterial strains was maintained at −50 but not at −8 kPa. The narrowness of the sand particle size distribution allows calculating the average thickness of the liquid film found around the sand grains, following the derivations in ref *32*. The estimates obtained were 11.6, 4.9, and 1.2 μm at −1, −8, and −50 kPa, respectively. Previous results have shown that KT2440 swimming motility is very restricted in water films thinner than about 1.5 μm on average (*18*). This would explain why no extensive dispersal was observed at −50 kPa. Nevertheless, the difference in colonization rate between the wild type and nonflagellated mutant was modest, considering the 3 orders of magnitude difference between Brownian diffusion coefficient of a nonmotile strain (2×10^{-9} cm^2 s^{-1}) and random motility coefficients of swimming microorganisms ($2-19 \times 10^{-6}$ cm^2 s^{-1}) (*33*). Admittedly, these values were derived for bulk liquid and not for porous media (*34*) or for unsaturated media, but qualitative observations of KT2440 and a uncharacterized nonmotile mutant on an unsaturated surface also pointed toward larger differences in dispersal rate when the effective liquid film exceeds 1.5 μm (*18*). In addition to motility, microbial growth also contributed to the colonization of the microcosms as it has been previously observed in other experimental systems such as saturated porous media (*35*) or unsaturated surfaces (*18*). The difference between the dispersal rates presented here and those of ref *18* might primarily originate from differences in the geometry of hydrated pathways in a 3-D porous medium and on a 2-D surface.

If a number of observations support the hypothesis that chemotacic motility can contribute to aquifer bioremediation (*36, 37*), such a role in unsaturated soil has rarely been explored (*38*). Here, the microcosms inoculated with the nonmotile mutant displayed modestly but significantly reduced mineralization rates (Figure 2). This demonstrates the potential value of flagellar motility in the bioremediation of contaminated unsaturated matrices sufficiently moist to allow bacterial swimming. Nevertheless, our data also indicate that in wet and nutrient-rich matrices significant dispersal could also occur for nonflagellated cells, albeit at a smaller rate than for their flagellated counterparts.

Relevance to Field Conditions. Obviously, care must be taken to extrapolate our findings to real soils where several mechanisms can interfere with the mass transfer processes considered here. Many processes can impede bacterial dispersal, reinforcing the role of initial degrader distribution on mineralization rate. These include (i) the low connectivity and high tortuousity of most soils compared to our sand matrix, making bacterial dispersal slower than observed here (*19*), (ii) the presence of predators, which are considered responsible for the low survival of introduced microbes not embedded in a protective carrier (*39*), and (iii) the limited bacterial growth due to low concentrations of pollutant and/or electron acceptors (*40*). Symmetrically, other processes would potentially accelerate microbial migration. For example, our microcosms did not contain plant roots or fungi that are potentially able to mobilize degrader cells (*15*). Similarly, water infiltration, which was not considered here, is known to both enhance bacterial transport (*41*) and contribute to the transport of soluble pollutants (*42*). Because of the multiple mechanisms influencing bacterial and solute mass transfers, predicting the duration of diffusion limitation caused by the spatial separation of degraders and pollutant remains a difficult exercise.

For the engineer interested in bioremediating a soil, our work demonstrates that in dry soils it is necessary to consider the spatial separation between pollutant and degrading organisms as a barrier to mineralization. If bioaugmentation is chosen as a remediation strategy, the practitioner can adapt the mode of degrader delivery (free cells or carriers, number of carriers per unit volume of soil) as well as soil mixing in order to achieve reasonable distances between pollutant and degraders. We are currently working on determining the quantities of carriers necessary to achieve a desired mineralization rate as a function of soil hydration. Alternatively, some techniques exist that can force the migration of pesticide or degrading cells without direct mixing (*43*).

Acknowledgments

This work was funded by the Villum Kann Rasmussen Foundation Center of Excellence, Center for Environmental and Agricultural Microbiology (CREAM). B.F.S. is supported by the Marie Curie Excellence Grant MEXT-CT-2005-024004. Support from the French Embassy in Denmark is also gratefully acknowledged. We thank Julie Chambon and Mads Troldborg (DTU) for assistance with the modeling.

Supporting Information Available

Additional descriptions of the three bacterial distributions, procedures leading to the creation of the nonflagellated mutant, and the mathematical model are presented as well as graphs showing model sensitivity. This information is available free of charge via the Internet at http://pubs.acs.org/.

Literature Cited

(1) Grundmann, S.; Fu, R.; Schmid, M.; Laschinger, M.; Ruth, B.; Schulin, R.; Munch, J. C.; Schroll, R. Application of microbial hot spots enhances pesticide degradation in soils. *Chemosphere* **2007**, *68* (3), 511–517.

(2) Bazot, S.; Lebeau, T. Effect of immobilization of a bacterial consortium on diuron dissipation and community dynamics. *Bioresour. Technol.* **2009**, *100* (18), 4257–4261.

(3) Dechesne, A.; Pallud, C.; Bertolla, F.; Grundmann, G. L. Impact of the microscale distribution of a *Pseudomonas* strain introduced into soil on potential contacts with indigenous bacteria. *Appl. Environ. Microbiol.* **2005**, *71* (12), 8123–8131.

(4) Ritz, K.; McNicol, W.; Nunan, N.; Grayston, S.; Millard, P.; Atkinson, D.; Gollotte, A.; Habeshaw, D.; Boag, B.; Clegg, C. D.; Griffiths, B. S.; Wheatley, R. E.; Glover, L. A.; McCaig, A. E.; Prosser, J. I. Spatial structure in soil chemical and microbiological properties in an upland grassland. *FEMS Microbiol. Ecol.* **2004**, *49* (2), 191–205.

(5) Grundmann, G. L.; Debouzie, D. Geostatistical analysis of the distribution of $NH4^+$ and $NO2^-$-oxidizing bacteria and serotypes at the millimeter scale along a soil transect. *FEMS Microbiol. Ecol.* **2000**, *34* (1), 57–62.

(6) Grundmann, G. L.; Dechesne, A.; Bartoli, F.; Flandrois, J. P.; Chasse, J. L.; Kizungu, R. Spatial modeling of nitrifier microhabitats in soil. *Soil Sci. Soc. Am. J.* **2001**, *65* (6), 1709–1716.

(7) Vinther, F. P.; Brinch, U. C.; Elsgaard, L.; Fredslund, L.; Iversen, B. V.; Torp, S.; Jacobsen, C. S. Field-scale variation in microbial activity and soil properties in relation to mineralization and sorption of pesticides in a sandy soil. *J. Environ. Qual.* **2008**, *37* (5), 1710–1718.

(8) Muller, K.; Smith, R. E.; James, T. K.; Holland, P. T.; Rahman, A. Spatial variability of atrazine dissipation in an allophanic soil. *Pest Manag. Sci.* **2003**, *59* (8), 893–903.

(9) Rasmussen, J.; Aamand, J.; Rosenberg, P.; Jacobsen, O. S.; Sørensen, S. R. Spatial variability in the mineralisation of the phenylurea herbicide linuron within a Danish agricultural field: multivariate correlation to simple soil parameters. *Pest Manag. Sci.* **2005**, *61* (9), 829–837.

(10) Pallud, C.; Dechesne, A.; Gaudet, J. P.; Debouzie, D.; Grundmann, G. L. Modification of spatial distribution of 2,4-dichlorophenoxyacetic acid degrader microhabitats during growth in soil columns. *Appl. Environ. Microbiol.* **2004**, *70* (5), 2709–2716.

(11) Vieublé Gonod, L.; Chadoeuf, J.; Chenu, C. Spatial distribution of microbial 2,4-dichlorophenoxy acetic acid mineralization from field to microhabitat scales. *Soil Sci. Soc. Am. J.* **2006**, *70* (1), 64–71.

(12) Cho, J. C.; Tiedje, J. M. Biogeography and degree of endemicity of fluorescent *Pseudomonas* strains in soil. *Appl. Environ. Microbiol.* **2000**, *66* (12), 5448–5456.

(13) Holden, P. A.; Firestone, M. K. Soil microorganisms in soil cleanup: How can we improve our understanding. *J. Environ. Qual.* **1997**, *26*, 32–40.

(14) Harms, H.; Bosma, T. N. P. Mass transfer limitation of microbial growth and pollutant degradation. *J. Ind. Microbiol. Biotechnol.* **1997**, *18* (2−3), 97–105.

(15) Kohlmeier, S.; Smits, T. H. M.; Ford, R. M.; Keel, C.; Harms, H.; Wick, L. Y. Taking the fungal highway: Mobilization of pollutant-degrading bacteria by fungi. *Environ. Sci. Technol.* **2005**, *39* (12), 4640–4646.

(16) Monard, C.; Martin-Laurent, F.; Vecchiato, C.; Francez, A. J.; Vandenkoornhuyse, P.; Binet, F. Combined effect of bioaugmentation and bioturbation on atrazine degradation in soil. *Soil Biol. Biochem.* **2008**, *40* (9), 2253–2259.

(17) Parkin, T. B.; Shelton, D. R. Spatial and temporal variability of carbofuran degradation in soil. *J. Environ. Qual.* **1992**, *21* (4), 672–678.

(18) Dechesne, A.; Or, D.; Gülez, G.; Smets, B. F. The porous surface model: A novel experimental system for online quantitative observation of microbial processes under unsaturated conditions. *Appl. Environ. Microbiol.* **2008**, *74*, 5195–5200.

(19) Gammack, S. M.; Paterson, E.; Kemp, J. S.; Cresser, M. S.; Killham, K. Factors Affecting the Movement of Microorganisms in Soils. In *Soil Biochemistry*; Stotzky, G., Bollag, J., Eds.; Marcel Dekker: New York, 1992; Vol. 7, pp 263−305.

(20) Hu, Q.; Wang, J. S. Y. Aqueous-phase diffusion in unsaturated geologic media: A review. *Crit. Rev. Environ. Sci. Technol.* **2003**, *33* (3), 275.

(21) Teruko, N. Travels of a *Pseudomonas*, from Japan around the world. *Environ. Microbiol.* **2002**, *4* (12), 782–786.

(22) Quenee, L.; Lamotte, D.; Polack, B. Combined *sacB*-based negative selection and *cre-lox* antibiotic marker recycling for efficient gene deletion in *Pseudomonas aeruginosa*. *Biotechniques* **2005**, *38* (1), 63–67.

(23) Hansen, S. K.; Haagensen, J. A. J.; Gjermansen, M.; Jorgensen, T. M.; Tolker-Nielsen, T.; Molin, S. Characterization of a *Pseudomonas putida* rough variant evolved in a mixed-species biofilm with *Acinetobacter* sp strain C6. *J. Bacteriol.* **2007**, *189* (13), 4932–4943.

(24) Bashan, Y. Alginate beads as synthetic inoculant carriers for slow release of bacteria that affect plant growth. *Appl. Environ. Microbiol.* **1986**, *51* (5), 1089–1098.

(25) Treves, D. S.; Xia, B.; Zhou, J.; Tiedje, J. M. A two-species test of the hypothesis that spatial isolation influences microbial diversity in soil. *Microbial Ecol.* **2003**, *45* (1), 20–28.

(26) Harris, R. F. Effect of Water Potential on Microbial Growth and Activity. In *Water Potential Relations in Soil Microbiology*; Parr, J. F., Gardner, W. R., Elliot, L. F., Eds; Soil Science Society of America: Madison, WI, 1981; pp 23−95.

(27) Olesen, T.; Moldrup, P.; Henriksen, K.; Petersen, L. W. Modeling diffusion and reaction in soils 0.4. New models for predicting ion diffusivity. *Soil Sci.* **1996**, *161* (10), 633–645.

(28) Holden, P. A.; Halverson, L. J.; Firestone, M. K. Water stress effects on toluene biodegradation by *Pseudomonas putida*. *Biodegradation* **1997**, *8* (3), 143–51.

(29) Bosma, T. N. P.; Middeldorp, P. J. M.; Schraa, G.; Zehnder, A. J. B. Mass transfer limitation of biotransformation: Quantifying bioavailability. *Environ. Sci. Technol.* **1997**, *31* (1), 248–252.

(30) Harms, H. Bacterial growth on distant naphthalene diffusing through water, air, and water-saturated and nonsaturated porous media. *Appl. Environ. Microbiol.* **1996**, *62* (7), 2286–2293.

(31) Hall, B. M.; McLoughlin, A. J.; Leung, K. T.; Trevors, J. T.; Lee, H. Transport and survival of alginate-encapsulated and free *lux-lac* marked *Pseudomonas aeruginosa* UG2Lr cells in soil. *FEMS Microbiol. Ecol.* **1998**, *26* (1), 51–61.

(32) Schaefer, C. E.; Arands, R. R.; Vandersloot, H. A.; Kosson, D. S. Prediction and experimental validation of liquid-phase diffusion resistance in unsaturated soils. *J. Contam. Hydrol.* **1995**, *20* (1−2), 145–166.

(33) Berg, H. C. *Random Walks in Biology*. Princeton University Press: Princeton, NJ, 1993.

(34) Ford, R. M.; Harvey, R. W. Role of chemotaxis in the transport of bacteria through saturated porous media. *Adv. Water Resour.* **2007**, *30* (6−7), 1608–1617.

(35) Sharma, P. K.; McInerney, M. J.; Knapp, R. M. In situ growth and activity and modes of penetration of *Escherichia coli* in unconsolidated porous materials. *Appl. Environ. Microbiol.* **1993**, *59* (11), 3686–3694.

(36) Marx, R. B.; Aitken, M. D. Bacterial chemotaxis enhances naphthalene degradation in a heterogeneous aqueous system. *Environ. Sci. Technol.* **2000**, *34* (16), 3379–3383.

(37) Wang, M.; Ford, R. M.; Harvey, R. W. Coupled effect of chemotaxis and growth on microbial distributions in organic-amended aquifer sediments: Observations from laboratory and field studies. *Environ. Sci. Technol.* **2008**, *42* (10), 3556–3562.

(38) Paul, D.; Singh, R.; Jain, R. K. Chemotaxis of *Ralstonia* sp. SJ98 towards *p*-nitrophenol in soil. *Environ. Microbiol.* **2006**, *8* (10), 1797–1804.

(39) England, L. S.; Lee, H.; Trevors, J. T. Bacterial survival in soil: Effect of clays and protozoa. *Soil Biol. Biochem.* **1993**, *25* (5), 525–531.
(40) van Veen, J. A.; van Overbeek, L. S.; van Elsas, J. D. Fate and activity of microorganisms introduced into soil. *Microbiol Mol Biol Rev* **1997**, *61* (2), 121–135.
(41) Hekman, W. E.; Heijnen, C. E.; Trevors, J. T.; Van Elsas, J. D. Water-flow induced transport of *Pseudomonas fluorescens* cells through soil columns as affected by inoculant treatment. *FEMS Microbiol. Ecol.* **1994**, *13* (4), 313–326.
(42) McGrath, G. S.; Hinz, C.; Sivapalan, M. Modeling the effect of rainfall intermittency on the variability of solute persistence at the soil surface. *Water Resour. Res.* **2008**, *44*, (9).
(43) Harms, H.; Wick, L. Y. Dispersing pollutant-degrading bacteria in contaminated soil without touching it. *Eng. Life Sci.* **2006**, *6* (3), 252–260.

ES902760Y